JOURNAL OF SOLID STATE CHEMISTRY 109, 211–218 (1994)

Valence Charge Fluctuations in $Tl_{2-x-z}Ba_2Ca_{2+x}Cu_3O_{10-y}$ System

C. S. Gopinath and S. Subramanian[1]

Regional Sophisticated Instrumentation Centre, Indian Institute of Technology, Madras 600 036, India

and

M. Paranthaman and A. M. Hermann

Department of Physics, Campus Box 390, University of Colorado, Boulder, Colorado 80309

Received October 16, 1992; in revised form June 7, 1993; accepted June 14, 1993

Systematic XPS core level studies and wet chemical analysis in the $Tl_{2-x-z}Ba_2Ca_{2+x}Cu_3O_{10-y}$ system have been carried out for the "as synthesized" samples. Broadening of Ca 2*p* core level and ionic radii considerations suggest that calcium substitutes at the Tl site. The valence state of thallium in Tl2223 is between +3 and +1, and substitution of calcium at thallium site oxidizes thallium to Tl(III) to optimize the hole concentration and maximize T_c. Origin of holes in this system is discussed in terms of charge transfer between Tl (or Tl, Ca) and CuO_2 layers. The Cu $2p_{3/2}$ core level shows that the relative intensity of satellite, the energy separation between main line and the satellite and binding energy of main line varies in a systematic way. The observed variations are explained with a simplified configuration interaction model. An increase in charge transfer energy and a decrease in hybridization strength is predicted for higher Ca substitution.

I. INTRODUCTION

Soon after the discovery of high-temperature superconductivity in the Tl–Ba–Ca–Cu–O system by Sheng and Hermann (1), many phases with high critical temperature have been reported. It is now clear that the highest critical temperature, T_c of 127 K can be obtained only in the $Tl_2Ba_2Ca_2Cu_3O_{10}$ (referred as Tl2223) phase (2). It has been suggested in the literature that part of the Ca substitutes on the Tl site (3, 4). Liu *et al.* (5) and Dong *et al.* (6) have reported recently that by using Ca-rich starting compositions, one can conveniently prepare Tl2223 phase. Very recently Paranthaman *et al.* (7) studied the system $Tl_{2-x-z}Ba_2Ca_{2+x}Cu_3O_{10-y}$ (*z* and *y* represent Tl and O vacancies respectively) to determine Tl and O contents and oxidation of Cu above the formal valence Tl(III) or hole concentration (n_h). Goodenough and co-workers (8, 9) have already established simple wet chemical procedures to determine the Tl and O content in Tl-based cuprate superconductors. It is now well understood (9) that in the double Tl–O layer superconductors the Tl 6*s* band overlaps that of the CuO_2 sheets at the Fermi energy (E_F).

Only a few reports on Tl-based superconductors are available about its electronic structure as determined by various high-energy spectroscopic studies (10–13). Recently, we have reported (14) the XPS studies of valence state of Tl in single TlO layered $TlBa_{1-x}Sr_xLaCuO_5$ ($0 \leq x \leq 1$) system and explained the appearance of superconductivity with higher Sr concentration as mainly due to the overlap of Tl 6*s* and $\sigma^*_{x^2-y^2}$ bands at E_F. There are various mechanisms of generation of holes in *p*-type high T_c superconductors. They can be created by substitution of higher valency elements by lower valency elements, by excess oxygen, charge transfer, cation vacancy, order–disorder phenomena, etc. In particular an increase in Tl substitution by Ca in Tl2223 phase increases the n_h in the CuO_2 layers and increases the T_c also without affecting the lattice parameters appreciably (7). These observations suggest that the increase in n_h in this system is due to both Tl-6*s* band overlap with the conduction band and Ca(II) substitution on the Tl sites. What happens to the Tl(I) present in Tl2223, which is largely responsible for Tl 6*s* and $\sigma^*_{x^2-y^2}$ overlap, upon substitution of Tl by Ca is not yet explained.

Undoped cuprates are insulators of the charge transfer type. The upper Hubbard band is based on $3d_{x^2-y^2}$ orbitals of Cu and has a partial O 2*p* character due to covalency. Upon doping, by one of the processes mentioned above, a hole impurity-like band is formed at the top of a bonding band, which finally merges with the valence band to build a partially filled conduction band. This model of the O 2*p* character of hole carriers is supported by different high energy spectroscopic studies (12, 15–16). This "ligand-

[1] To whom correspondence should be addressed.

0022-4596/94 $6.00

hole" formalism allows one to understand how the charge transfer from CuO_2 to TlO layers can occur when the Tl 6*s* band crosses the Fermi level. However, this model has to be refined to account for all the spectroscopic results.

Prominent satellite structure observed in Cu(II) compounds by X-ray photoelectron spectroscopy (XPS) in Cu 2*p* core levels has been interpreted in terms of charge fluctuation and strong coulombic interaction between a core hole and the localized valence *d* orbitals. Sawatzky and co-workers (17, 18) have successfully explained the variation of the metal 2*p* satellite intensity with main line intensity (I_s/I_m) using a simplified configuration interaction (CI) model for Cu and Ni dihalides. It was recently demonstrated that the relative intensity of the satellite in the Cu 2*p* of $YBa_2Cu_3O_{7-x}$ (YBCO) (19), $La_{2-x}Sr_xCuO_4$, family of Bi and Tl cuprates (20), and of $Bi_2Sr_2Ca_{1-x}Y_xCu_2O_{8+y}$ (21), is related to the charge-transfer energy and n_h. Even though the CI model is highly simplified, it appears to give a consistent trend with existing experimental data such as I_s/I_m and energy separation between main line and the satellite (*W*).

In the present paper, Tl 4*f*, Ca 2*p*, and Cu $2p_{3/2}$ core level XPS are studied to probe the $Tl_{2-x-z}Ba_2Ca_{2+x}Cu_3O_{10-y}$ system. The results on the undoped compounds and those with slight excess Ca confirm the creation of holes in CuO_2 layers due to both the overlap of Tl 6*s* and antibonding $\sigma^*_{x^2-y^2}$ bands and to direct doping effects of Ca(II) on Tl(III) sites. However, for $x \geq 0.4$, the results presented here show that the holes are created only by the latter doping effect.

II. EXPERIMENTAL

The compounds $Tl_{2-x-z}Ba_2Ca_{2+x}Cu_3O_{10-y}$ (Tl2223) were synthesized by a high-temperature solid state reaction method and preparation details were published elsewhere (7). Only "as synthesized" samples were used for all the measurements. The samples were characterized by X-ray powder diffraction. Superconductive transition temperatures were obtained as the diamagnetic onset temperature measured with a commercial DC SQUID magnetometer under a field of 0.01 T (Fig. 1). The Tl and O contents were determined by wet chemical procedures reported by Paranthaman and co-workers (8, 9). The n_h were determined by assuming all Tl to be in oxidation state III (22).

XPS measurements were made with a VG ESCALAB MkII spectrometer equipped with Mg$K\alpha$ X-ray source (1253.6 eV). The overall resolution of the spectrometer is better than 0.7 eV. All the binding energies (BE) are referenced to the adventitious C 1*s* peak at 285.0 eV. Samples are scraped *in situ* with a steel blade inside the analysis chamber prior to the measurements under high vacuum of better than 10^{-9} Torr. Accuracy of all BE values are ±0.1 eV. Only two samples ($x = 0.0$ and 0.3) showed contamination to a small extent due to carbon, which may be due to unreacted carbonates. Our XPS data of $x = 0.0$ compound, which are in good agreement with literature (10, 11), suggest that our results are not affected by carbon contamination. Since these samples have well-known surface contamination problems (formation of $BaCO_3$ and $Ba(OH)_2$ on surface), we have taken maximum care to minimize the effects by scraping the sample thoroughly over the surface with a stainless steel blade *in situ* under high vacuum. The observation of a clear metallic edge at E_F on these samples depends on the surface contamination as well. Recently Arko *et al.* (23) reported photoemission studies at 20 K and room temperature (RT) on YBCO to address this problem. However, for core level XPS, the results are not affected and low-temperature results are reproduced at RT also (23). Moreover, we have observed (data not shown) a Fermi edge for all samples suggesting the purity of our surface and its metallic character.

III. RESULTS AND DISCUSSION

(i) Structure, Superconductivity, and Wet Chemical Analysis

Single phase $Tl_{2-x-z}Ba_2Ca_{2+x}Cu_3O_{10-y}$ samples were obtained in the composition range $0 \leq x \leq 0.4$. For $x = 0.6$, a small $Tl_{0.2}Ca_{0.8}CuO_y$ impurity phase is formed. All samples have been indexed on the basis of a tetragonal structure. The lattice parameters, *a* and *c*, are nearly constant for all samples with the value of 3.858 ± 0.002 Å and 35.71 ± 0.01 Å, respectively, giving strong evidence that the Tl2223 phase forms in the region $0 \leq x \leq 0.4$. Systematic changes have been observed in the photoemission studies and T_c with *x*. Since all the samples are prepared under identical conditions, we believe the T_c changes observed are really due to the substitution of Ca(II) for Tl.

Figure 1 shows the temperature dependence of dc susceptibility for all the samples studied. The T_c varies between 112 and 118 K for the as synthesized samples $0 \leq x \leq 0.6$ and are reported in Table 1. The samples with $x = 0.4$ gives the highest T_c of 118 K with a sharp transition. $x = 0.3$ gives a T_c of 116 K with relatively high Meissner fraction compared to other samples.

Wet chemical analysis data for all samples are reported along with T_c and lattice parameters in Table 1. All samples are deficient in both Tl and O contents. Both the n_h and T_c increase with *x*. The n_h for all the samples are between 0.11 and 0.19. These values appear to be low when compared to higher values (0.20 ± 0.02) expected for triple-CuO_2-layer superconductors with these critical temperatures (24, 25). Our XPS results of the BE of Tl $4f_{7/2}$ (refer to Fig. 3) in $x = 0.0$ is 118.1 eV, which is in

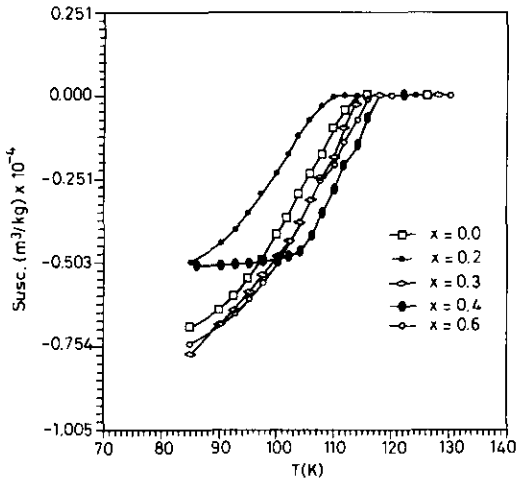

FIG. 1. Temperature dependence of dc susceptibility for the "as synthesized" $Tl_{2-x-z}Ba_2Ca_{2+x}Cu_3O_{10-y}$ samples (zero-field cooled).

between the BE of Tl_2O_3 (117.7 eV) and Tl_2O (118.7 eV). These results clearly indicate that there is some Tl 6*s* band overlap with the conduction band of the CuO_2 sheets due to the presence of mixed valency +3 and +1 thallium, and a consequent increase instead of reduction in the observed n_h. The Tl–Tl near neighbor interaction in all these samples will be lower compared to that in other double Tl-layer compounds such as $Tl_2Ba_2CuO_6$, since some of the Ca substitutes onto the Tl site. This narrows the Tl 6*s* band and reduces the Tl 6*s* band overlap with $\sigma^*_{x^2-y^2}$ bands. Further Ca substitution onto the Tl site produces some additional holes. Hence, the origin of increased n_h (oxidation of CuO_2 sheets) in some of these samples ($x \leq 0.3$) may be due to Tl 6*s* band overlap with the conduction band of the CuO_2 sheets on the one hand and Ca substituting on the Tl sites on the other, the latter being more probable in $x \geq 0.4$ samples.

We mention again here that we have assumed an oxidation state III for Tl and calculated the Cu oxidation state and hence n_h. This does not mean that there is no Tl 6*s* band overlap with $\sigma^*_{x^2-y^2}$. Hence the actual hole concentration variation is more than what we have reported here and in our earlier report (7). Because of the simplifying assumptions that have to be made in the analysis of n_h, it may not be correct to calculate the valency of Tl from the data in Table 1 and hence the actual hole concentration.

(ii) Ca 2p Core Level XPS

XPS studies have been carried out at RT on the $Tl_{2-x-z}Ba_2Ca_{2+x}Cu_3O_{10-y}$ system. Figure 2 shows the Ca 2*p* core level spectra of the compounds with $x = 0.0$, 0.3, and 0.4. As the Ca concentration is increased the 2*p* core level broadens. The extent of broadening is such that both spin orbit levels could not be resolved for $x \geq 0.4$. The full width at half maximum (FWHM) for sample with $x = 0.0$ is 2.4 eV, $x = 0.3$ is 3.1 eV and is greater than 3.5 eV for $x \geq 0.4$ samples. This enormous broadening with increasing x suggests that there should be at least two entirely different chemical species of Ca(II) in this system. In the $x = 0.0$ sample, some of the calcium is at the Tl site (3, 4). The ionic radii consideration of various ions also suggest that Ca^{2+} (1.12 Å) substitutes only at Tl^{3+} (1.00 Å) site, but not at Ba^{2+} (1.47 Å) or at Cu^{2+} (0.73 Å) sites. The electronic environment in Ca and Tl sites is entirely different. The Ca sites, which are between the CuO_2 sheets, are completely oxygen depleted and the one at the Tl site is surrounded by six oxygens in an octahedral coordination. We have deconvoluted the Ca 2*p* core level spectrum of the $x = 0.4$ sample, with a program developed in our laboratory (26), to show the presence of two different overlapping components. The higher BE spin orbit levels are assigned to the Ca at Tl site due to octahedral oxygen coordination, and the lower BE spin orbit levels are assigned to the Ca at the actual Ca site, mainly on the basis of the oxygen depleted nature of this layer.

TABLE 1
Analytical Data for $Tl_{2-x-z}Ba_2Ca_{2+x}Cu_3O_{10-y}$

Nominal starting composition	Lattice parameters		Analytical data*			T_c (K) (±1 K)
	a (Å)	*c* (Å)	Tl content	oxygen content (10 − *y*)	n_a[a]	
$Tl_2Ba_2Ca_2Cu_3O_{10}$	3.859(2)	35.72(2)	1.78	9.83	0.107	114
$Tl_{1.8}Ba_2Ca_{2.2}Cu_3O_{10-y}$	3.861(4)	35.76(3)	1.66	9.92	0.153	112
$Tl_{1.7}Ba_2Ca_{2.3}Cu_3O_{10-y}$	3.858(2)	35.71(2)	1.52	9.82	0.160	116
$Tl_{1.6}Ba_2Ca_{2.4}Cu_3O_{10-y}$	3.856(2)	35.72(2)	1.33	9.67	0.183	118
$Tl_{1.4}Ba_2Ca_{2.6}Cu_3O_{10-y}$	3.857(2)	35.70(2)	1.10	9.53	0.187	118

* Error bar involved is ±0.01

[a] All Tl is assumed to be in the oxidation state III.

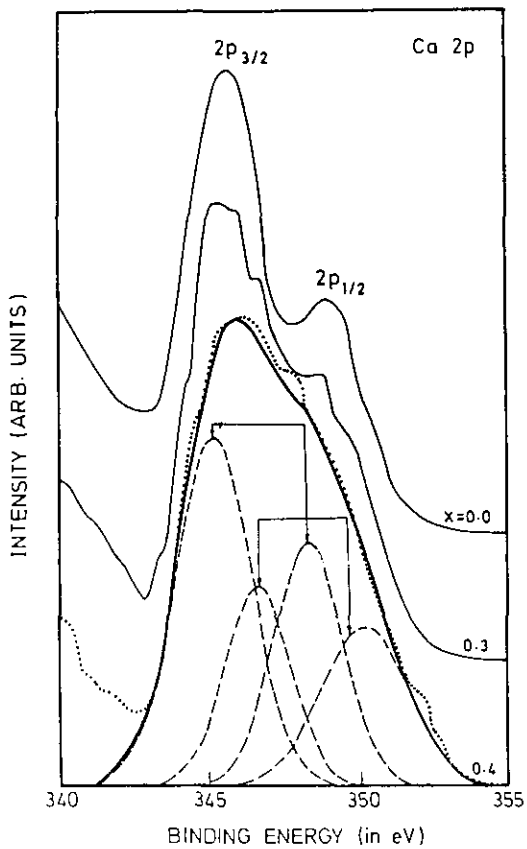

FIG. 2. Calcium $2p$ core level spectra of $Tl_{2-x-z}Ba_2Ca_{2+x}Cu_3O_{10-y}$ for $x = 0.0$, 0.3, and 0.4. Note the broadening and increase in FWHM of the spectra as x increases. The $x = 0.4$ spectrum is deconvoluted (broken line curves) and the spin-orbit doublets are indicated by arrow marks. The dotted line is the experimental spectrum for $x = 0.4$.

Substitution of Ca at the Tl site increases the n_h, which we have observed in our wet chemical analysis. The increase in n_h and the similar values of the lattice parameters with increasing x cannot be accounted for if Ca substitutes at Ba and/or Cu site, which is isovalent to that of Ca. But the n_h in the system increases with x. This may be due to the oxidation of all Tl ions to Tl(III) which will be explained in the following section.

(iii) Tl 4f Core Level XPS

XPS of Tl $4f$ core levels had been studied by McGuire *et al.* (27) in Tl_2O_3 and some Tl(I) compounds. BE of the $4f_{7/2}$ level in Tl(I) compounds are observed to be higher (BE varies between 118.7 and 119.4 eV depending on the anions) than that of Tl_2O_3 (117.7 eV) is consistent with the results of McGuire *et al.* (see Fig. 3). The Tl $4f$ core level XPS collected from freshly scraped surfaces of samples with $x = 0.0$ to 0.6 are shown in Fig. 3.

There is a clear trend in the variation of these spectra as Ca concentration changes. First the BE of $4f_{7/2}$ line varies from 118.1 eV at $x = 0.0$ and 0.2, 117.9 at $x = 0.3$, 117.7 at $x = 0.4$, to 118.1 eV at $x = 0.6$. The FWHM of the $4f_{7/2}$ line varies from 2.2 eV at $x = 0.0$–0.4 to 2.45 eV at $x = 0.6$. These results clearly indicate that there is some Tl $6s$ band overlap with the conduction band of the CuO_2 sheets, i.e., due to the presence of mixed valency +3 and +1 or reduced valence state of Tl at least in $x \leq 0.3$. But for $x = 0.4$ the BE is 117.7 eV, which is equal to that of Tl_2O_3, suggests that all Tl is in the +3 oxidation state. From these observations we conclude that substitution of Ca at Tl oxidizes all the Tl ions to Tl(III). The substitution of Ca(II) for Tl(III) definitely increases the n_h in this system; at the same time presence of reduced valence state of Tl also increases the n_h. If this is true a very high n_h would have been predicted. However, the n_h obtained from wet chemical analysis is still lower than that expected for the triple-CuO_2-layer system (24, 25). This can be explained only with the oxidation of all Tl to Tl(III) progressively with increasing x having an optimum n_h and achieving higher T_c. It is clear from the Ca $2p$ spectra and wet chemical analysis results that the variation in Tl $4f$ BE is not only due to Tl vacancies but also due to the substitution of Ca at the Tl site.

In the case of $x = 0.6$ the BE of the overall peak is at

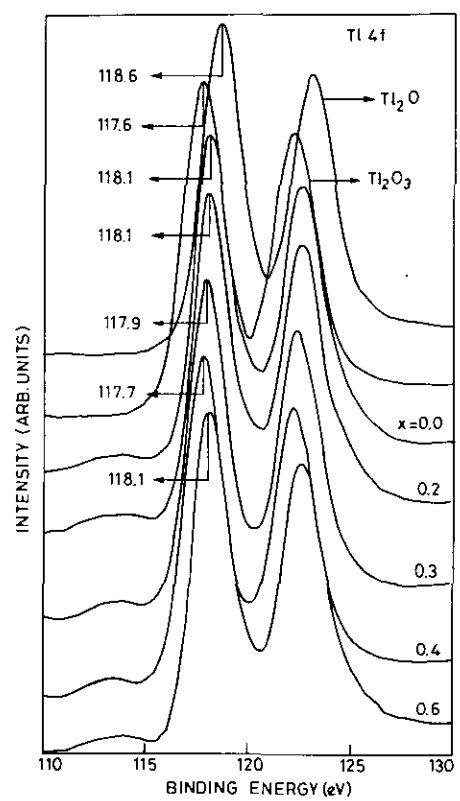

FIG. 3. Thallium $4f$ core level spectra for Tl_2O, Tl_2O_3, and $Tl_{2-x-z}Ba_2Ca_{2+x}Cu_3O_{10-y}$ (x values are indicated). Note the broadening of the spectrum for $x = 0.6$ alone.

118.1 eV. This is not due to the mixed valency and it is attributed to the impurity phase ($Tl_{0.2}Ca_{0.8}CuO_y$) present in this particular sample (7). This is further supported from the observation of broadening of Tl 4*f* core levels (FWHM is 2.45 eV) for $x = 0.6$ alone. The Tl–Tl near neighbor interaction in all these samples will be lower as compared to that in other double-TlO-layer compounds, due to Ca substitution at Tl site. This could be another reason for the broadening of core levels. But the broadening is observed only for $x = 0.6$ excluding the latter possibility and is caused by the impurity phase.

As we progressively increase the Ca substitution onto Tl site, all the Tl oxidizes to Tl(III) and the Tl 6*s* band narrows in width, decreasing the overlap between the Tl 6*s* and $\sigma^*_{x^2-y^2}$ bands. In other words, the double-Tl-layer compound approaches the nature of single-Tl-layer compounds in terms of overlap at E_F with the $\sigma^*_{x^2-y^2}$ bands, as we increases the Ca substitution. An increase in the n_h, corresponding to a lowering of Fermi level and an increase in density of states (DOS), leads to an increase in T_c within weak-coupling BCS theory (28), as is observed experimentally. Our XPS results on undoped samples ($x = 0.0$) are in agreement with Marksteiner *et al.* (29) and the XPS measurements of Meyer *et al.* (10).

(iv) Cu $2p_{3/2}$ Core Level XPS

The Cu $2p_{3/2}$ core level XPS spectra, collected from freshly scraped surfaces of samples with $x = 0.0$ to 0.6 are shown in Fig. 4a. They are composed of two components with a main line at a BE of around 933 eV and a satellite between 938 and 948 eV due to a well screened final state ($Cu2p^53d^{10}\underline{L}$), where $\underline{L}$ denotes the holes on the surrounding ligands, and an unscreened ($Cu2p^53d^9$) final state respectively. The I_s/I_m ratios are obtained from the areas under the satellite and main line (after background subtraction) and the satellite to main line separations (W) are obtained from the energy differences between the centroids of the two peaks. The satellite intensity is directly proportional to the pure d^9 species. There is a clear trend in the variations of these spectra as calcium concentration changes. The BE of main line varies from 932.7 eV at $x = 0.0$, 933.3 eV at $x = 0.2$, 932.8 eV at $x = 0.3$, 933.1 eV at $x = 0.4$, and to 933.5 eV at $x = 0.6$. The intensity of the satellite peak increases continuously and the energy separation W decreases continuously with x. I_s/I_m increases from 0.24 to 0.40 and W decreases from 9.4 to 8.8 eV. Although this shift is not quite obvious from Fig. 3a, a quantitative analysis shows a clear trend in the variation of I_s/I_m and W with x (Fig. 4b). Besides, the FWHM of main line also increases continuously from 2.7 eV at $x = 0.0$ to 3.6 eV at $x = 0.6$.

The observed variations are explained as follows. The low I_s/I_m and a BE value (932.7 eV) close to that of CuO

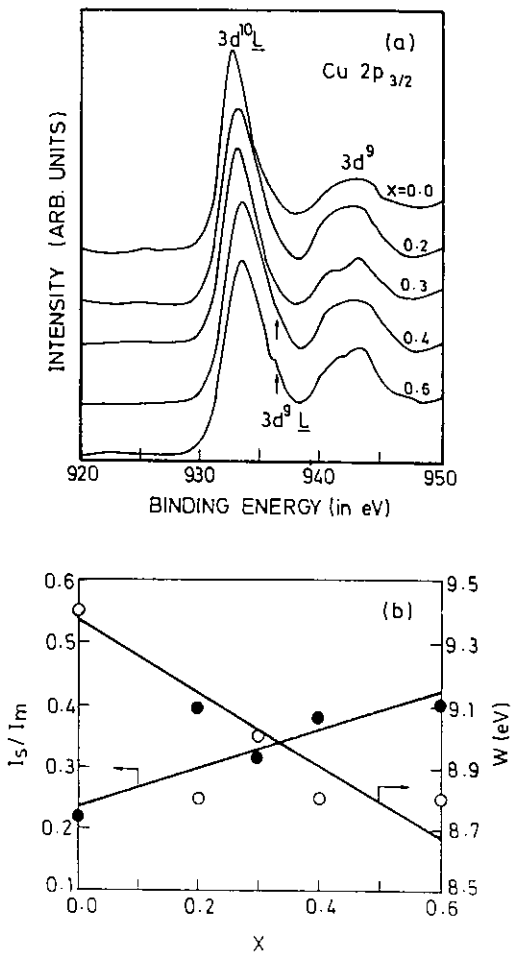

FIG. 4. (a) Copper $2p_{3/2}$ core level spectra of $Tl_{2-x-z}Ba_2Ca_{2+x}Cu_3O_{10-y}$ (x values are indicated). Note the contribution of $d^9\underline{L}$ configuration for $x = 0.4$ and 0.6 (arrow mark) and extension of the satellite at higher BE for $x = 0.6$. (b) Variation of satellite to main line intensity (I_s/I_m) and energy separation between the main line and satellite (W) plotted against x. Solid lines are guides to the eye.

(933.0 eV) for $x = 0.0$ suggest that more amount of $d^{10}\underline{L}$ configuration contributes to the ground level system. As we increase the Ca substitution, holes are supplied to the system, and the hole concentration increases with T_c. This suggests that more amount of d^9 species produced from $d^{10}\underline{L}$ species, and as a result of this the satellite intensity also increases. Increase in BE of the main line is due to the conversion of $d^{10}\underline{L}$ to d^9, $d^9\underline{L}$, d^8, and $d^{10}\underline{L}^2$. It is likely that the d^8 component is excluded from the ground state because of its 10 eV excitation energy relative to the E_F (30) and the weight of $d^{10}\underline{L}^2$ is likely to be very small because of the double excitation on the ligand. In comparison with the BE of main line of $LaCuO_3$ (936.7 eV) (31), where Cu is in a +3 oxidation state, we can safely assume that there is no contribution of $d^9\underline{L}$ or it may be below the detection level for $x = 0.0$-0.3. But in

x = 0.4 and 0.6, a clear hump (marked by an arrow) is seen at the higher BE (936 eV) side, indicating the contribution of $d^9\underline{L}$ state. Moreover, the tail of the satellite, which is above the background level, extends up to a BE of 947 eV, which is a characteristic feature of Cu(III) compounds (31–32), in the x = 0.6 compound. This suggests that more and more $d^9\underline{L}$ components are formed at higher Ca substitution and it should lead to a decrease in hybridization strength (τ), since $d^9\underline{L}$ ground state energy is higher than that of $d^{10}\underline{L}$, d^9 and O $2p^6$. All of these processes can be easily explained with increase in hole concentration. However, this cannot explain the decrease in W. Moreover the n_h is only 0.187 for x = 0.6, which is below the expected value for the triple-CuO_2-layer system. To explain these features, we associate the evolution of different ground state configurations of the Cu(II) with the observed Cu $2p_{3/2}$ spectra in Fig. 3. This change is related to the redistribution of holes between Cu and O atoms, when the Tl ions are replaced by Ca with the introduction of oxygen deficiency in the lattice. We have not considered any $d^9\underline{L}$ contribution to our calculations. We mention here that the Cu(II) and Cu(III) states are not mixed in the final states, since the τ is zero (33).

A sudden increase in BE and I_s/I_m of x = 0.2 compound is observed, differing from the overall trend (Fig. 4b). This is mainly attributed to the higher oxygen content found in this sample. The higher oxygen content increases the n_h and hence d^9 species. But the same n_h for x = 0.0 and 0.2 suggests that only the d^9 species is produced from $d^{10}\underline{L}$.

We interpret our results presented here in terms of the CI model (17–21). Three important energy parameters are considered here; the charge transfer energy (Δ), defined as ε_p-ε_d, the $2p$ core hole to d-hole repulsion energy (U_{dc}), and the hybridization strength between the Cu $3d$ and O $2p$ derived states (τ or transfer integral). The eigen states in the ground state are described by the CI of two symmetrized states: $|Cu3d^9\rangle$ and $|Cu3d^{10}\underline{L}\rangle$. The latter state represents the charge transfer state. The final states observed in the photoemission are the linear combinations of symmetrized $|Cu\ 2p^53d^9\rangle$ and $|Cu\ 2p^53d^{10}\underline{L}\rangle$. Figure 5a shows an energy level diagram of the configurations included in treating the ground state and the states reached in $2p$ photoemission, with the effect of hybridization. For the detailed description of the model, the reader is referred to Ref. (17).

The two experimentally observed parameters I_s/I_m and W depend on three unknowns namely, Δ, τ, and U_{dc}. In order to explain the experimental results, reasonable ranges of these can be assumed and the resulting calculated I_s/I_m and W can be compared with the experiment. In Fig. 5b we have plotted the values of I_s/I_m and W ($2p$) as a function of Δ for three different values of τ = 2, 2.5, and 3.0. U_{dc} is fixed at 8 eV in all the calculations. The

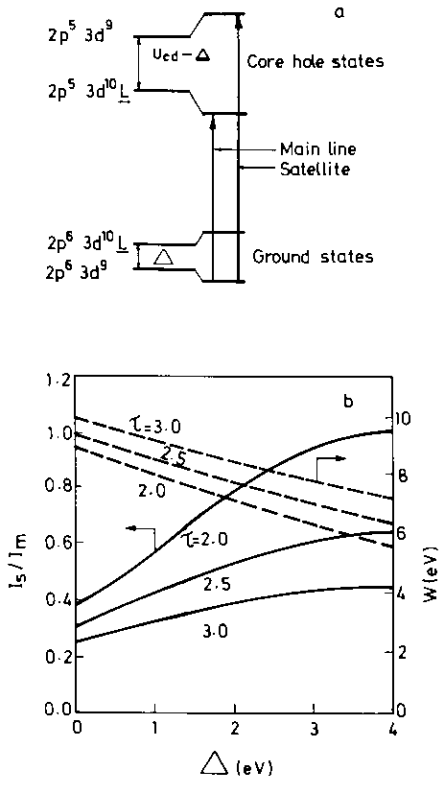

FIG. 5. (a) Energy level diagram for configurations of the cluster model description of the initial and final states for Cu $2p$ XPS. The changes in splittings are due to hybridization. (b) Satellite to main line intensity (I_s/I_m), and energy separation between main line and satellite (W) calculated using configuration interaction (CI) model are plotted against charge transfer energy (Δ) in the range of 0 to 4 eV for three different transfer integral values (τ = 2.0, 2.5, and 3.0). U_{dc} is assumed to be 8.0 eV throughout the calculations (see text).

highly simplified, nevertheless realistic, CI model reproduces the experimental results satisfactorily. Our calculation of I_s/I_m of Tl2223 with x = 0.0 to 0.6 show that: (1) the value of Δ increases continuously with x and (2) decrease in τ is responsible for the increase in I_s/I_m. Greater formation of $d^9\underline{L}$ components also points to a decrease in τ, which is in good agreement with the calculations. Even if we choose the typical values for high T_c cuprates, with $\Delta \approx$ 1–2 eV, τ = 2 eV, and $U_{dc} \approx$ 7.8–8.5 eV, these parameters result in values of I_s/I_m which fall to the left hand side of the curves in Fig. 5b. When a larger number of different configurations contribute to the ground state, the energy of the lowest eigen state goes down and the energy gap between main line and satellite increases. But in the present system due to the increase in n_h, a large amount of the d^9 species is produced from $d^{10}\underline{L}$, which should lead to a decrease in energy gap between the main line and satellite. On the other hand, the energy gap between the ground states is decreased and the lower energy eigen state tends toward the d^9 energy

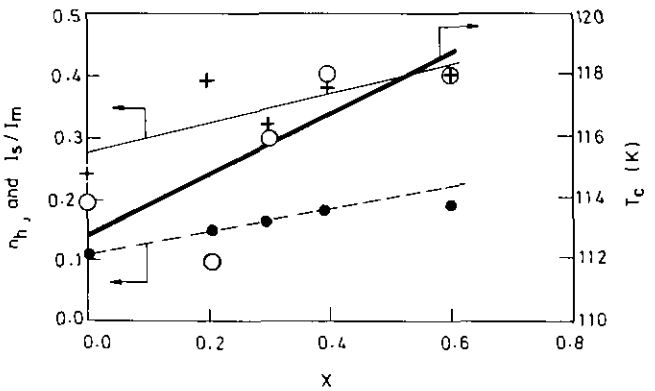

FIG. 6. Hole concentration n_h (closed circles and broken line), T_c (open circles and thick line), and I_s/I_m (plus symbols and thin line) are plotted versus x. Note the direct correlation between x and n_h, T_c, and I_s/I_m (see text). Lines are guides to the eye.

due to the higher d^9 contribution. This explains our experimental observations of an increase in BE of the Cu $2p_{3/2}$ main line. Therefore if I_s/I_m increases as x increases in Tl2223, W should decrease at the same time, as is observed experimentally (Fig. 4b).

In Fig. 6 we show the plots of T_c, n_h, and I_s/I_m in $Tl_{2-x-z}Ba_2Ca_{2+x}Cu_3O_{10-y}$ system versus x. We notice an increase in T_c, n_h, and I_s/I_m with x. These plots demonstrate easily how n_h and I_s/I_m vary monotonically with x. But here we would like to caution the reader that exactly the opposite trend is observed for $Bi_2Sr_2Ca_{1-x}Y_xCu_2O_{8+y}$ system (21). When more Ca is introduced into the Tl2223 system to yield a higher T_c with higher n_h, the associated changes in the electronic structure of Cu–O show an increase of Δ and decrease of τ. In conclusion we suggest, I_s/I_m is directly proportional to Δ and it need not necessarily depend on n_h nor on T_c.

IV. CONCLUSIONS

Single phase Tl2223 compounds, pristine and Ca-for-Tl substituted, have been synthesized and characterized. A systematic increase in n_h and T_c is observed. We have presented the detailed core level XPS studies of Ca $2p$, Tl $4f$, and Cu $2p_{3/2}$. Ca $2p$ core level XPS show a broadening with x due to occupation of Tl site by Ca. Occupation of Tl sites by Ca also oxidizes all Tl to Tl(III) progressively. Tl $4f$ core level studies also support the above conclusion. Mixed valent character of Tl is shown in compounds with lower x (≤ 0.3). We have observed variations in the Cu $2p$ spectra with x. Simplified CI model calculations are carried out to explain the observed experimental results. The calculations indicate an increase in Δ and a decrease in τ as Ca concentration increases.

ACKNOWLEDGMENTS

C.S.G. would like to thank NSTB-DST, New Delhi for the award of a National Superconductivity Fellowship. At the University of Colorado at Boulder, we gratefully acknowledge the support of office of Naval Research under ONR Grant N000 14-90-J-1571.

REFERENCES

1. Z. Z. Sheng and A. M. Hermann, *Nature* **332,** 55 (1988); ibid., *Nature* **332,** 138 (1988).
2. S. S. P. Parkin, V. Y. Lee, E. M. Engler, A. I. Nazzal, T. C. Huang, G. Gorman, R. Savoy, and R. Beyers, *Phys. Rev. Lett.* **60,** 2539 (1988).
3. D. E. Cox, C. C. Torardi, M. A. Subramanian, J. Gopalakrishnan, and A. W. Sleight, *Phys. Rev. B* **38,** 6624 (1988).
4. A. W. Sleight, *Science* **242,** 1519 (1988).
5. R. S. Liu, J. D. Johnson, P. P. Edwards, and A. M. Campbell, *Solid State Commun.* **79,** 43 (1991).
6. C. Dong, H. M. Duan, W. Kiehl, A. Nazirpour, J. W. Drexler, and A. M. Hermann, *Physica C* **196,** 291 (1992).
7. M. Paranthaman, M. Foldeaki, and A. M. Hermann, *Physica C* **192,** 161 (1992) and references therein.
8. M. Paranthaman, A. Manthiram, and J. B. Goodenough, *J. Solid State Chem.* **87,** 479 (1990).
9. A. Manthiram, M. Paranthaman, and J. B. Goodenough, *Physica C* **171,** 135 (1990).
10. H. M. Meyer III, T. J. Wagener, J. H. Weaver, and D. S. Ginley, *Phys. Rev. B* **39,** 7343 (1989).
11. T. Suzuki, M. Nagoshi, Y. Fukuda, Y. Syono, M. Kikuchi, N. Kobayashi, and M. Tachiki, *Phys. Rev. B* **40,** 5184 (1989).
12. F. Studer, N. Merrien, C. Martin, C. Michel, B. Raveau, and A. Fontaine, *Physica C* **178,** 324 (1991).
13. A. Krol, C. S. Lin, Y. L. Soo, Z. H. Ming, Y. H. Kuo, Jui H. Wang, Min Qi, and G. C. Smith, *Phys. Rev. B* **45,** 10051 (1992).
14. A. Sundaresan, C. S. Gopinath, A. S. Tamhane, A. K. Rajarajan, M. Sharon, S. Subramanian, R. Pinto, L. C. Gupta, and R. Vijayaraghavan, *Phys. Rev. B,* **46,** 6622 (1992).
15. J. Fink, N. Nucker, M. Alexander, H. Romberg, M. Knupfer, M. Merkel, P. Adelmann, R. Claessen, G. Mante, T. Buslaps, S. Harm, R. Manzke, and M. Skibowski, *Physica C* **185–189,** 45 (1991).
16. A Fujimori, Y. Tokura, H. Eisaki, H. Takagi, S. Uchida, and M. Sato, *Phys. Rev. B* **40,** 7303 (1989).
17. G. van der Laan, C. Westra, C. Haas, and G. A. Sawatzky, *Phys. Rev. B* **23,** 4369 (1981).
18. J. Zaanan, C. Westra, and G. A. Sawatzky, *Phys. Rev. B* **33,** 8060 (1986).
19. J.-J. Yeh, I. Lindau, J.-Z. Sun, K. Char, N. Missert, A. Kapitulnik, T. H. Geballe, and M. R. Beasley, *Phys. Rev. B* **42,** 8044 (1990).
20. C. N. R. Rao, G. Ranga Rao, M. K. Rajumon, and D. D. Sarma, *Phys. Rev. B* **42,** 1026 (1990).
21. C. S. Gopinath, S. Subramanian, P. Sumana Prabhu, M. S. R. Rao, G. V. Subba Rao, *Physica C* **218,** 117 (1993).
22. M. Paranthaman, A. Manthiram, and J. B. Goodenough, *J. Mater. Chem.* **2,** 317 (1992).
23. A. J. Arko, R. S. List, R. J. Bartlett, S.-W. Cheong, Z. Fisk, J. D. Thompson, C. G. Olson, A.-B. Yang, R. Liu, C. Gu, B. W. Veal, J. Z. Liu, A. P. Paulikas, K. Vandervoort, H. Claus, J. C. Campuzano, J. E. Schirber, and N. D. Shinn, *Phys. Rev. B* **40,** 2268 (1989).
24. A. Manthiram, M. Paranthaman, and J. B. Goodenough, *J. Solid State Chem.* **96,** 464 (1992).
25. C. N. R. Rao, J. Gopalakrishnan, A. K. Santra, and V. Manivannan, *Physica C* **174,** 11 (1991).

26. G. V. R. Chandramouli, S. Lalitha, and P. T. Manoharan, *Comput. Chem.* **14,** 257 (1990).
27. G. E. McGuire, G. K. Schweitzer, and T. A. Carlson, *Inorg. Chem.* **12,** 2450 (1973).
28. J. Bardeen, L. N. Cooper, and J. R. Schrieffer, *Phys. Rev.* **108,** 1175 (1957).
29. P. Marksteiner, Jaejun Yu, S. Massidda, A. J. Freeman, J. Redinger, and P. Weinberger, *Phys. Rev. B* **39,** 2894 (1989).
30. M. R. Thuler, R. L. Benbow, and Z. Hurick, *Phys. Rev. B* **26,** 669 (1982).
31. K. Allan, Alan Campion, J. Zhou, and J. B. Goodenough, *Phys. Rev. B* **41,** 11572 (1990).
32. A. Bianconi, A. Congiu Castellano, M. De Santis, P. Delogu, A. Gargano, and R. Giogi, *Solid State Commun.* **63,** 1135 (1987).
33. A. Balzarotti, M. De Crescenzi, N. Motta, F. Patella, and A. Sgarlata, *Phys. Rev. B* **38,** 6461 (1988).